Journal of Pharmaceutical and Biomedical Analysis 277 (2026) 117510

Contents lists available at ScienceDirect

Journal of Pharmaceutical and Biomedical Analysis

journal homepage: www.journals.elsevier.com/journal-of-pharmaceutical-and-biomedical-analysis

Targeted phytocannabinomics provides new insights into the biosynthetic origin of *cis*-Δ⁹-THCA in *Cannabis sativa* L.

Luca Buccolieri [a,b,*], Roberta Paris [c], Flavia Fulvio [c], Ilaria Alberti [d], Cinzia Citti [b,e,**], Giuseppe Cannazza [b,e]

[a] Department of Physics and Astronomy, Vrije Universiteit Amsterdam, De Boelelaan 1081, Amsterdam 1081 HV, Netherlands
[b] Institute of Nanotechnology – CNR NANOTEC, Campus Ecotekne, Via Monteroni, Lecce 73100, Italy
[c] CREA – Research Centre for Cereal and Industrial Crops, Via di Corticella 133, Bologna 40128, Italy
[d] CREA – Research Centre for Cereal and Industrial Crops, Via G. Amendola 82, Rovigo 45100, Italy
[e] Department of Life Sciences, University of Modena and Reggio Emilia, Via G. Campi 103, Modena 41125, Italy

ARTICLE INFO

Keywords:
Cannabis sativa L.
HPLC-HRMS
Cis-tetrahydrocannabinolic acid
Phytocannabinoids
Chemotype

ABSTRACT

Recent studies have reported the occurrence of *cis*-Δ⁹-tetrahydrocannabinol (*cis*-Δ⁹-THC) and its carboxylated precursor, *cis*-Δ⁹-tetrahydrocannabinolic acid (*cis*-Δ⁹-THCA), minor isomers of the well-known *trans* counterparts. However, their origin remains unclear and several hypotheses have been proposed. In this work, *cis*-Δ⁹-THCA and the major phytocannabinoids, including cannabidiolic acid (CBDA), *trans*-Δ⁹-tetrahydrocannabinolic acid (*trans*-Δ⁹-THCA), cannabichromenic acid (CBCA), and their biosynthetic precursor cannabigerolic acid (CBGA), were quantified in a large and diverse set of *C. sativa* accessions using a targeted metabolomics approach based on liquid chromatography coupled to high-resolution Orbitrap mass spectrometry (HPLC-HRMS). Our findings indicate that *cis*-Δ⁹-THCA does not appear to be chemically derived from other cannabinoids, prompting new considerations regarding its biosynthetic origin. Notably, growth-stage analyses revealed a parallel accumulation pattern between *cis*-Δ⁹-THCA and CBCA, suggesting the potential involvement of CBCA synthase in its formation. Overall, this study provides new evidence on the distribution, variability, and possible biosynthetic pathways of *cis*-Δ⁹-THCA, enriching current understanding of cannabinoid diversity in *C. sativa*.

1. Introduction

Cannabis sativa L. is one of the most widely discussed plant species, as its inflorescences represent the most commonly used recreational drug worldwide, yet the plant also has a long history in traditional Chinese medicine and in the fiber industry of Western countries. In recent years, renewed interest in its potential applications has emerged, spanning clinical use [1–5] as well as environmentally sustainable technologies, building materials, and agri-food innovation [6,7].

Both the psychoactive and therapeutic properties of *C. sativa* are attributed to phytocannabinoids, a peculiar class of terpenophenolic metabolites naturally produced in their carboxylated forms. Their biosynthesis involves the reaction between a resorcinol and an isoprenoid moiety, with structural variability accounting for more than 150 phytocannabinoids described to date [8–12]. Among the most abundant compounds featuring a pentyl side chain, cannabigerolic acid (CBGA) acts as the central precursor from which three major cannabinoids, namely cannabidiolic acid (CBDA), Δ⁹-tetrahydrocannabinolic acid (Δ⁹-THCA), and cannabichromenic acid (CBCA), are enzymatically produced through distinct oxidocyclases (Fig. 1). Upon exposure to heat or light, these acidic forms undergo decarboxylation to yield the corresponding neutral species: cannabidiol (CBD), *trans*-Δ⁹-tetrahydrocannabinol (*trans*-Δ⁹-THC), and cannabichromene (CBC), respectively.

Phytocannabinoid profiles are commonly used to classify *C. sativa* chemotypes, defined according to the relative ratio between THC, CBD, and CBG, where the total amount of each cannabinoid in both its acidic and neutral forms is taken into account. Five chemotypes have been described [13], namely: chemotype I (THC/CBD higher than 10), chemotype II (THC/CBD ratio close to 1), chemotype III (THC/CBD ratio

* Corresponding author at: Department of Physics and Astronomy, Vrije Universiteit Amsterdam, De Boelelaan 1081, Amsterdam 1081 HV, Netherlands.
** Correspondence to: Institute of Nanotechnology of the National Council of Research – CNR NANOTEC, Campus Ecotekne, Via Monteroni, Lecce 73100, Italy.
E-mail addresses: l.buccolieri@vu.nl (L. Buccolieri), cinzia.citti@cnr.it (C. Citti).

https://doi.org/10.1016/j.jpba.2026.117510
Received 3 February 2026; Received in revised form 26 March 2026; Accepted 10 April 2026
Available online 11 April 2026

lower than 1), chemotype IV (CBG predominant varieties), chemotype V (negligible phytocannabinoids levels). These chemotypic fingerprints area a valuable insight in the underlying genotypes and offer valuable information for breeding programs and geographic origin studies [14].

Among phytocannabinoids, *trans*-Δ⁹-THC is the most extensively studied due to its well-established psychoactive properties. Owing to the presence of two stereogenic centers (C6*a* and C10*a*), four stereoisomers of Δ⁹-THC are possible: (–)-*trans*-Δ⁹-THC, (+)-*trans*-Δ⁹-THC, (–)-*cis*-Δ⁹-THC, and (+)-*cis*-Δ⁹-THC. In their acidic forms (Fig. 2), only (–)-*trans*-Δ⁹-THCA was known to occur naturally, and evidence regarding trace amounts of the (+)-*trans* isomer remains inconclusive [15–17].

The natural occurrence of *cis* isomers within the THC family has long been debated. The first report of *cis*-Δ⁹-THC in *C. sativa* dates back to 1976 [18], but subsequent studies focused primarily on the neutral forms generated upon heating plant material prior to analysis. Since carboxylated phytocannabinoids are thermolabile, analytical workflows relying on gas chromatography inherently promote decarboxylation and may lead to artefactual formation of *cis*-Δ⁹-THC. More recently, the presence of *cis*-Δ⁹-THCA in unheated plant extracts was confirmed [19]. Notably, two chemotype III samples in that study exhibited higher levels of *cis*-Δ⁹-THCA, closer to those of the *trans* isomer in chemotypes III and IV.

Smith and Kempfert [18] also reported that plants with a high CBD/THC ratio (chemotype III) showed higher amounts of *cis*-Δ⁹-THC, often with *trans/cis* ratios of 1:1 or 2:1, whereas THC-dominant varieties displayed ratios exceeding 10:1. These findings were later supported by Schafroth *et al.* [20], who additionally demonstrated that *cis*-Δ⁹-THC occurs as a scalemic mixture in plant material.

Several hypotheses have been proposed to explain the origin of *cis*-Δ⁹-THCA and its corresponding neutral derivative. Early work by Uliss *et al.* [21] and Razdan and Zitko [22] suggested chemical isomerization involving intermediate CBD isomers. Later, Schafroth *et al.* [20] proposed two possibilities: (i) the action of a dedicated oxidocyclase, analogous to known cannabinoid synthases, or (ii) a pericyclic cyclization mechanism related to the formation of CBCA from CBGA (Fig. 1).

Given that sample heating can generate artefactual products, elucidating the true phytocannabinoid composition *in planta* requires analytical workflows that avoid thermal degradation. In this study, leveraging access to a pure analytical standard of *cis*-Δ⁹-THCA, we quantify this recently characterized phytocannabinoid alongside CBGA, CBDA, *trans*-Δ⁹-THCA, and CBCA using a validated HPLC-HRMS method. Our large dataset of 97 samples from multiple accessions and chemotypes provides a robust foundation to explore potential relationships between *cis*-Δ⁹-THCA and other phytocannabinoids, and to investigate hypotheses regarding its biosynthetic origin.

2. Materials and methods

2.1. Materials

A total of 97 *Cannabis sativa* inflorescence samples from 40 different genotypes were included in this study. Inflorescences were harvested at full maturity from open-field cultivated plants and dried at 30–35 °C for 48–72 h. Most samples (n = 69) derived from commercial varieties propagated by seed. Specifically, eight chemotype III varieties (Codimono, Carmaleonte, Carmagnola, Eletta Campana, Fibranova, Fibrante, Futura 75, and CS) and one chemotype IV variety (Felsinea, currently under registration in the Italian Register of Varieties) were collected as

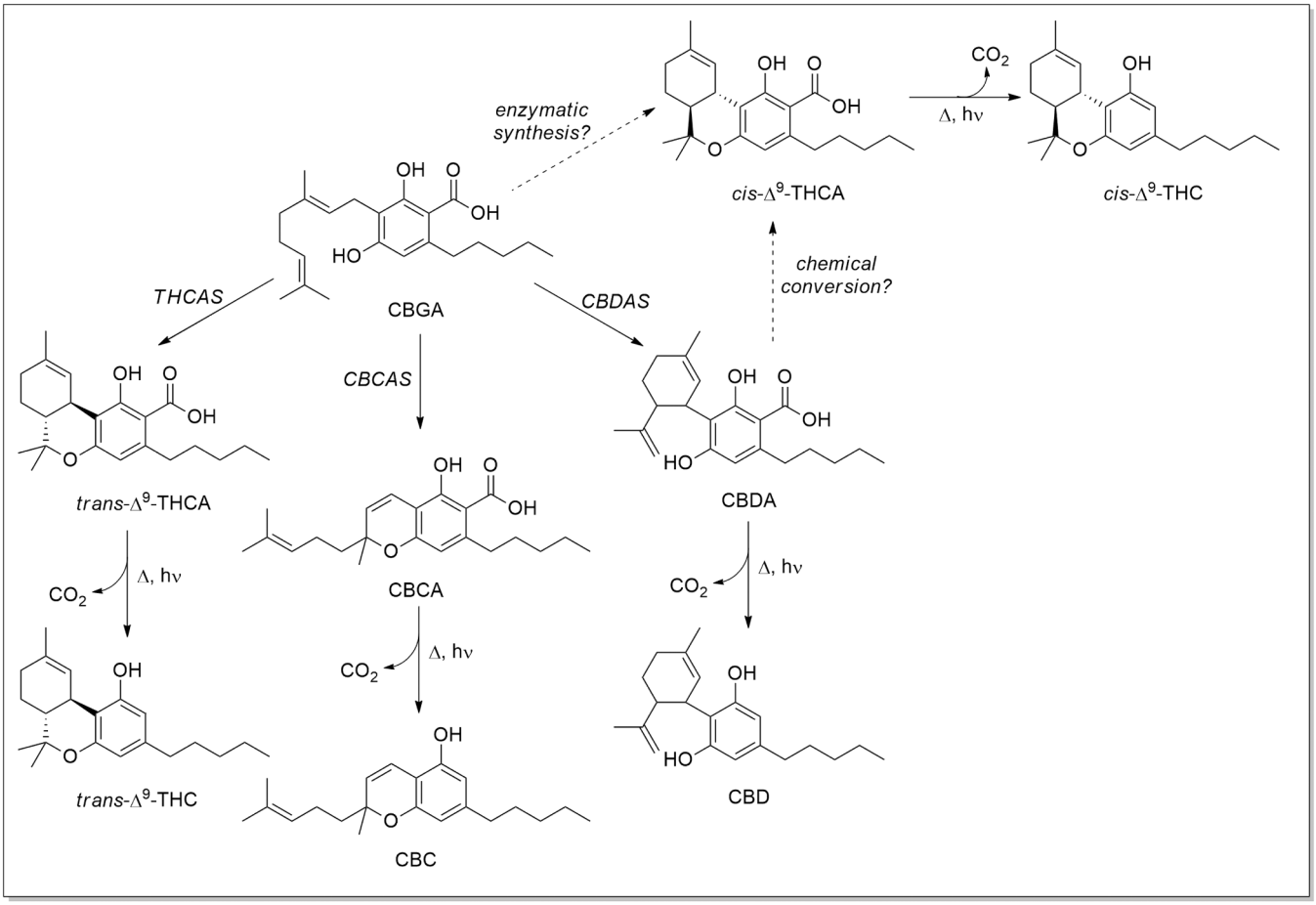

Fig. 1. Phytocannabinoids biosynthesis. Biosynthetic pathway of the main phytocannabinoids through specific synthases and decarboxylation driven by heat or light exposure.

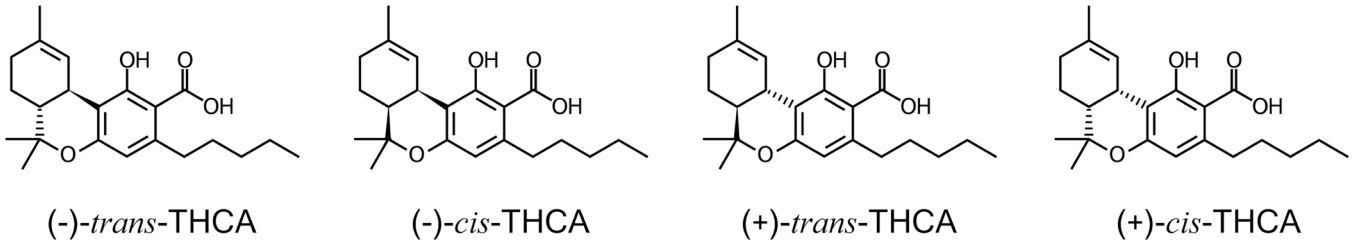

Fig. 2. THCA stereoisomers. Chemical structure of the four possible THCA stereoisomers.

both apical flowers and 30 cm-long apical stems, with three biological replicates per matrix, for a total of six samples per variety.

For three additional chemotype III varieties (Fibror 79, Tiborszallasi, Secuieni Jubileum), only apical flowers were collected, each sample composed of a pooled mixture of nine inflorescences. Twelve Finola single-female plants previously characterized for chemotype [23] were also included: five chemotype II plants and seven chemotype III plants. An additional 11 samples (labelled "S" followed by a number) were derived from landraces and seed-propagated lines, each collected as a single sample except for S1172, which was collected in replicate. Finally, 16 samples labelled "V" (V2–6, V9, V12–15, V18, V20–24) originated from a clonally (rooted cuttings) maintained collection of elite genotypes. All lines and landraces were taken from a germplasm collection of CREA and were already characterized for chemical profiles of mature inflorescences.

To investigate biosynthetic trends during early development, 12 additional samples were obtained from seedlings belonging to chemotypes I, II, and III. Samples were collected across early BBCH growth [24] stages: 09 (cotyledons and hypocotyls), 11 (one true leaf pair), 12 (two leaf pairs), and 13 (three leaf pairs), with three biological replicates per stage.

Acetonitrile, analytical grade ethanol 96% (*v/v*), formic acid, and LC-MS grade water were purchased from Carlo Erba (Milan, Italy). Certified analytical standards of *trans*-Δ⁹-THCA, CBDA, CBCA, and CBGA were obtained from Cerilliant (Round Rock, TX, USA). Pure *cis*-Δ⁹-THCA was available from a recent synthesis [19].

2.2. Extraction of Cannabis sativa samples

A total of 109 plant samples were extracted following the monograph *Cannabis Flos* of the German Pharmacopoeia [25], as applied in previous studies [12,26,27].

Briefly, 500 mg of finely powdered biomass were subjected to three sequential extractions (15 min each) with 20 mL, 12.5 mL, and 12.5 mL of 96% ethanol. The combined extract was diluted to 50 mL with fresh ethanol in a volumetric flask. A 1 mL aliquot was filtered through a 0.45 μm syringe filter and diluted 1:10 with acetonitrile for HPLC-HRMS analysis.

2.3. Chromatographic and spectrometric methods

Phytocannabinoid separation and detection were performed using an HPLC-HRMS system (Vanquish Core, Thermo Fisher Scientific, Waltham, USA) equipped with a binary pump, vacuum degasser, thermostated autosampler (4 °C), thermostated column compartment (30 °C), and diode-array detector (DAD) operating at 270 and 306 nm. The DAD served solely for monitoring and not for quantification.

Chromatographic separation was achieved using a Poroshell 120 EC-C18 column (100 × 3.0 mm, 2.7 μm) equipped with a guard column (5 × 3.0 mm, 2.7 μm) maintained at 30 °C. Under the applied gradient conditions, *cis*-Δ⁹-THCA and *trans*-Δ⁹-THCA were baseline-separated, as confirmed by injection of pure *cis*- and *trans*-Δ⁹-THCA analytical standards along with an exemplary sample (Figure S1, Supplementary Information). The gradient elution program started from 95% solvent A (0.1% aqueous formic acid, *v/v*) and 5% solvent B (acetonitrile with 0.1% formic acid, *v/v*), linearly increasing to 95% B over 20 min and held for 3 min. A washing step at 98% B for 7 min was followed by column re-equilibration at initial conditions for 6 min. The flow rate was 0.5 mL/min, yielding a total runtime of 36 min [19].

The HPLC system was coupled to an Exploris 120 Orbitrap mass spectrometer (Thermo Fisher Scientific) with a heated electrospray ionization (HESI) source, operated in fast polarity switching mode (HESI+ and HESI–). Quantification of carboxylated cannabinoids was performed in negative ionization mode due to improved signal quality. HESI source parameters [19] were: capillary temperature 390 °C, vaporizer temperature 150 °C, electrospray voltage 4.2 kV (positive) and 3.8 kV (negative), sheath gas 55 a.u., auxiliary gas 5 a.u., S-lens RF level 45.

A combined acquisition method was employed, including full-scan (FS), data-dependent acquisition (DDA), and targeted selected ion monitoring (t-SIM) events within the same run. FS and DDA were used for untargeted metabolomics and MS/MS fragmentation, while t-SIM was applied to enhance sensitivity and selectivity for target phytocannabinoids. The parameters of the analyzer were as follows: FS resolution 60,000 FWHM (full width at half maximum) at *m/z* 200, DDA resolution 15,000 FWHM, scan range *m/z* 75–750, maximum injection time 54 ms (FS) and 22 ms (DDA), isolation window *m/z* 0.7 (FS) and 1.2 (DDA), stepped NCE (normalized collision energy) 20–40–100. In the t-SIM event the pseudo-molecular ions of the target analytes were isolated within a defined retention window (16.0–23.0 min): *m/z* (Δ*m/z* = 0.4) 357.2071 ($[M-H]^-$, $C_{22}H_{30}O_4$; CBDA, *trans*-Δ⁹-THCA, *cis*-Δ⁹-THCA, CBCA) and *m/z* 359.2228 ($[M-H]^-$, $C_{22}H_{32}O_4$; CBGA). Injection volume was 5 μL, and data were extracted using a 5-ppm mass tolerance.

Calibration curves were generated using eight points for CBDA, *trans*-Δ⁹-THCA, CBCA, and CBGA (0.01–50.0 μg/mL) and seven points for *cis*-Δ⁹-THCA (0.01–1.00 μg/mL). Additional matrix-matched calibration curves were prepared by spiking extracts of the low-cannabinoid variety Ermo.

2.4. Quantification of phytocannabinoids

Raw data were processed using Compound Discoverer 3.3 (Thermo Fisher Scientific), employing a modified "untargeted food research ID workflow without statistics" (Supplementary Information 1).

Quantitative data were exported and analysed using MetaboAnalyst 5.0 (Pang *et al.*, 2022). Five phytocannabinoids including CBDA, CBGA, CBCA, *trans*-Δ⁹-THCA, and *cis*-Δ⁹-THCA were treated as features for one-factor statistical and machine learning analyses.

Correlation analysis inside MetaboAnalyst was performed using Pearson correlation coefficients without prior rescaling of the data.

The linear regression fit on the relation between phytocannabinoids was performed using orthogonal distance regression (ODR), taking into account the standard deviation in both axis for each entry of the data set. For each fit, the value of the R^2 was adjusted for ODR fit and the 95% confidence interval was computed. For comparison between different ODR fits, z-statistic and p-value were extracted for each pair of regressions.

3. Results and discussion

3.1. Quantification of cis-Δ⁹-THCA in cannabis inflorescences

Using a metabolomics-oriented HPLC-HRMS workflow, we quantified *cis*-Δ⁹-THCA, cannabidiolic acid (CBDA), cannabigerolic acid (CBGA), *trans*-Δ⁹-tetrahydrocannabinolic acid (*trans*-Δ⁹-THCA), and cannabichromenic acid (CBCA) in a large and diverse set of *Cannabis sativa* samples derived from both drug-type and fiber-type plants. The t-SIM acquisition substantially improved the selectivity and specificity of the target analytes by excluding potential co-eluting compounds. Moreover, comparison of back-calculated concentrations obtained from pure standard solutions with those from matrix-matched calibration curves ruled out interfering peaks and confirmed the absence of significant matrix effects, in agreement with previous results [19]. Although the HESI source operated at elevated temperatures (390 °C), the analytes did not undergo thermal decomposition as electrospray ionization acts as a soft ionization process due to evaporative cooling. Moreover, no significant change in peak area was observed in either the samples or the analytical standard replicates, suggesting that no in-source isomerization occurred under the adopted conditions.

A total of 97 samples from 51 accessions were analysed using a previously validated HPLC-HRMS method (validation parameters are summarized in Table S1, Supplementary Information) [28]. The method showed high sensitivity (LOD 3 ng/mL; LLOQ 10 ng/mL), good linearity (R^2>0.995), and satisfactory precision (intra-day RSD 0.98–3.53%; inter-day RSD 4.92–7.71%), confirming its suitability for the quantification of *cis*-Δ⁹-THCA at low concentration levels. The two diastereomers *cis*- and *trans*-Δ⁹-THCA were baseline-separated under the applied chromatographic conditions and identified by comparison with analytical standards (Figure S1). No evidence of co-elution or peak distortion indicative of isomerization was observed.

As shown in Fig. 3a and reported in Table S2, the concentrations of the five quantified phytocannabinoids displayed marked variability both across chemotypes and among genotypes within the same chemotype. Nevertheless, the dominant phytocannabinoid in each sample consistently matched the chemotype classification. The concentrations of *cis*-Δ⁹-THCA varied widely, ranging from approximately 0.05–0.09 mg/g in chemotypes I, II, and IV to around 0.3 mg/g in chemotype III samples (Fig. 3b). Additionally, chemotype II samples exhibited considerable genotypic variability. Overall, chemotype III accessions displayed the highest *cis*-Δ⁹-THCA levels (Table S3).

Within chemotype III, two subgroups (IIIA and IIIB) were distinguishable based on the proportion of CBCA relative to the total quantified phytocannabinoids: subgroup IIIA showed CBCA levels approximately two-fold lower than subgroup IIIB (Figure S2a, Supplementary Information). Accordingly, *cis*-Δ⁹-THCA concentrations were, on average, twice as high in subgroup IIIB compared to subgroup IIIA (Figure S2b, Supplementary Information). This observation suggests a possible association between CBCA and *cis*-Δ⁹-THCA, which is further explored below.

3.2. Phytocannabinoid interrelations

To investigate the potential biosynthetic origin of *cis*-Δ⁹-THCA, correlation analyses were conducted across the five quantified phytocannabinoids. Hierarchical clustering (Fig. 4a) revealed two major groups: the first made of CBCA, CBDA, and *cis*-Δ⁹-THCA, and the second made of CBGA and *trans*-Δ⁹-THCA. The strongest correlation exhibited by *cis*-Δ⁹-THCA was observed with CBCA (r = 0.87), followed by CBDA

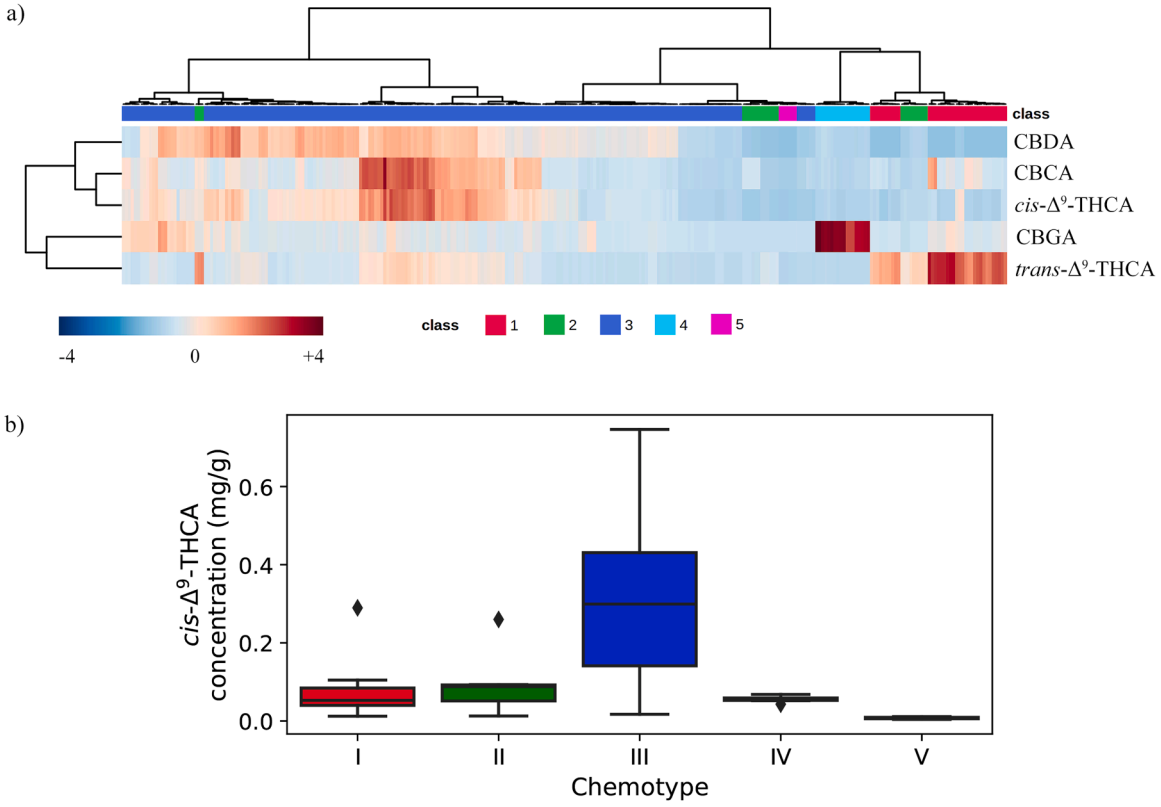

Fig. 3. *cis*-Δ^9-THCA is mainly present in chemotype III plants. Overview of the variability of 97 samples analysed through the HPLC-MS approach by a heatmap of the concentrations of 5 phytocannabinoids through the samples, with darker red tones indicating higher scores for the concentration and darker blue lower ones; each chemotype has a colour assigned as shown in the legend. Box and whisker chart representation of *cis*-Δ^9-THCA concentration among the different samples grouped according to the chemotype. The y axis shows the concentration of *cis*-Δ^9-THCA, expressed in mg/g. The average concentration of each series is marked by a cross inside each box while the range of the data is defined by the bars.

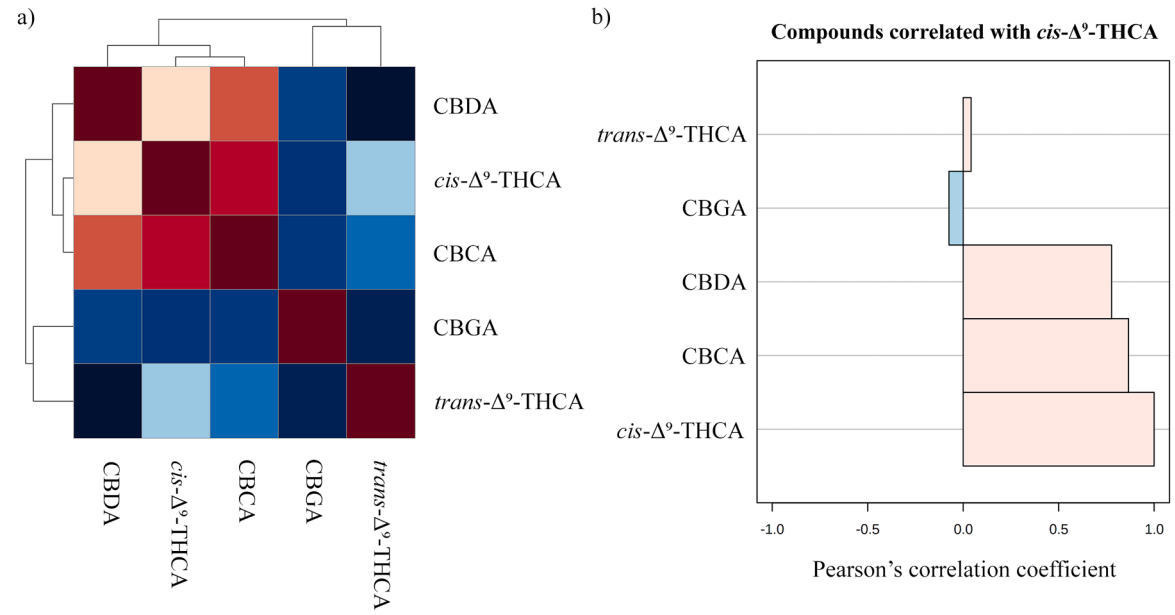

Fig. 4. *cis*-Δ^9-THCA concentration correlates with CBCA and CBDA presence. A correlation analysis was carried out using the five phytocannabinoids as features describing the dataset. Correlation heatmap of the features, clustered based on the correlation coefficient, with the score pairwise expressed in a blue-to-red (low-to-high) scale. Correlation histogram with *cis*-Δ^9-THCA as a reference.

(r = 0.78). Correlations with CBGA and *trans*-Δ⁹-THCA were negligible (< 0.1) (Fig. 4b; Table S4, Supplementary Information). CBCA also correlated moderately with CBDA (r = 0.50) and, to a lesser extent, with *trans*-Δ⁹-THCA (r = 0.27). These results indicate that *cis*-Δ⁹-THCA shares measurable relationships with cannabinoids derived from CBGA through specific oxidocyclases, while no direct relationship with the common precursor CBGA was observed. This behaviour, similar to that of CBDA, CBCA, and *trans*-Δ⁹-THCA, is consistent with a biosynthetic origin of *cis*-Δ⁹-THCA, although correlation alone does not establish causality.

Given these trends, pairwise cannabinoid relationships were examined with specific attention to chemotype-dependent behaviour.

CBGA, which represents the common precursor of CBDA, *trans*-Δ⁹-THCA, and CBCA, showed no meaningful correlation with any of these products, consistent with its further conversion through distinct oxidocyclases. Similarly, *cis*-Δ⁹-THCA showed no recognizable trend with CBGA (Fig. 5a). In contrast, *cis*-Δ⁹-THCA and CBCA concentrations displayed a clear linear trend in chemotype III samples (1/slope=59.42; R^2=0.75), while chemotype IV (1/slope=127.39; R^2=0.59) and II (1/slope=43.84; R^2=0.37) showed a lower fit quality (Fig. 5b). In contrast, chemotype I samples followed an independent and steeper trend (1/slope=332.11; R^2=0.74) (Fig. 5c).

For *cis*-Δ⁹-THCA and CBDA, chemotype-dependent behaviour was also observed. No clear trend was evident in chemotype I, while chemotype II samples showed a well-defined linear relationship (1/slope=138.78; R^2=0.79). In chemotypes III and IV, two distinct trends emerged (Fig. 5d), suggesting differences in metabolic regulation. The samples belonging to the group B of chemotype III showed a more pronounced increase in *cis*-Δ^9-THCA in relation to CBDA (1/slope=75.76; R^2=0.85) than the samples from group A (1/slope=153.61; R^2=0.78) and chemotype IV samples (1/slope=175.13; R^2=0.66), which showed no statistical difference.

In a similar fashion, *cis*-Δ⁹-THCA and *trans*-Δ⁹-THCA followed a single linear trend across most chemotypes, with correlations in chemotype I (1/slope=444.44; R^2=0.48) and IV (1/slope=30.70; R^2=0.51) and more robustly for chemotype II (1/slope=145.36; R^2=0.89) and group B of chemotype III (1/slope=20.96; R^2=0.86) (Fig. 5e). Interestingly, when the content of CBCA is low (group A of chemotype III), the linear relation between *cis* and *trans* isomers is lost. This would suggest that, without a relevant accumulation of CBCA, the synthesis of the two isomers of Δ^9-THCA is carried by two different pathways.

Because CBCA and *trans*-Δ⁹-THCA exhibited comparable behaviour in chemotypes III and IV, they were analysed together, showing a unified linear trend (1/slope=3.31; R^2=0.85) (Fig. 5f). Similarly, in chemotype II samples this relation is still preserved but with the opposite behavior (1/slope=0.25; R^2=0.84) in accordance with the higher *trans*-Δ^9-THCA content. Overall, these regressions should be considered descriptive and interpreted cautiously, as they may reflect shared regulatory or biosynthetic features rather than direct chemical relationships.

3.3. Ratio-based relationships among phytocannabinoids

To better understand how fluctuations in one phytocannabinoid relate to the ratios between others, additional analyses were performed. The CBDA/*cis*-Δ⁹-THCA ratio decreased as CBCA increased, following a parabolic trend, albeit with substantial dispersion at lower CBCA concentrations (<20 mg/g) (Fig. 6a). Chemotypes I and II deviated from this behaviour.

The ratios *trans*-Δ⁹-THCA/*cis*-Δ⁹-THCA and CBCA/*cis*-Δ⁹-THCA remained confined within relatively narrow ranges across most samples, regardless of CBDA concentration (Fig. 6b–c). Outliers included chemotypes I and II, as well as samples S1648, S1653, FINOLA 3, V4, and V5. Across the remaining samples, *trans*-Δ⁹-THCA/*cis*-Δ⁹-THCA ratios consistently ranged between 10 and 40, while CBCA/*cis*-Δ⁹-THCA between 20 and 85.

Collectively, these trends supported a potential biosynthetic connection between *cis*-Δ⁹-THCA and CBCA, suggesting possible involvement of CBCA synthase in the formation of *cis*-Δ⁹-THCA.

3.4. Phytocannabinoid production in seedlings

To further explore this relationship, phytocannabinoid accumulation was analysed during early developmental stages. CBCA synthase is predominantly expressed during the early developmental stages of *C. sativa* [29], and CBCA accumulates at higher concentrations in cotyledons and early leaves [30,31]. To explore whether *cis*-Δ⁹-THCA and CBCA share biosynthetic features, seedlings of chemotypes I, II, and III were analysed at BBCH stages 09, 11, 12, and 13.

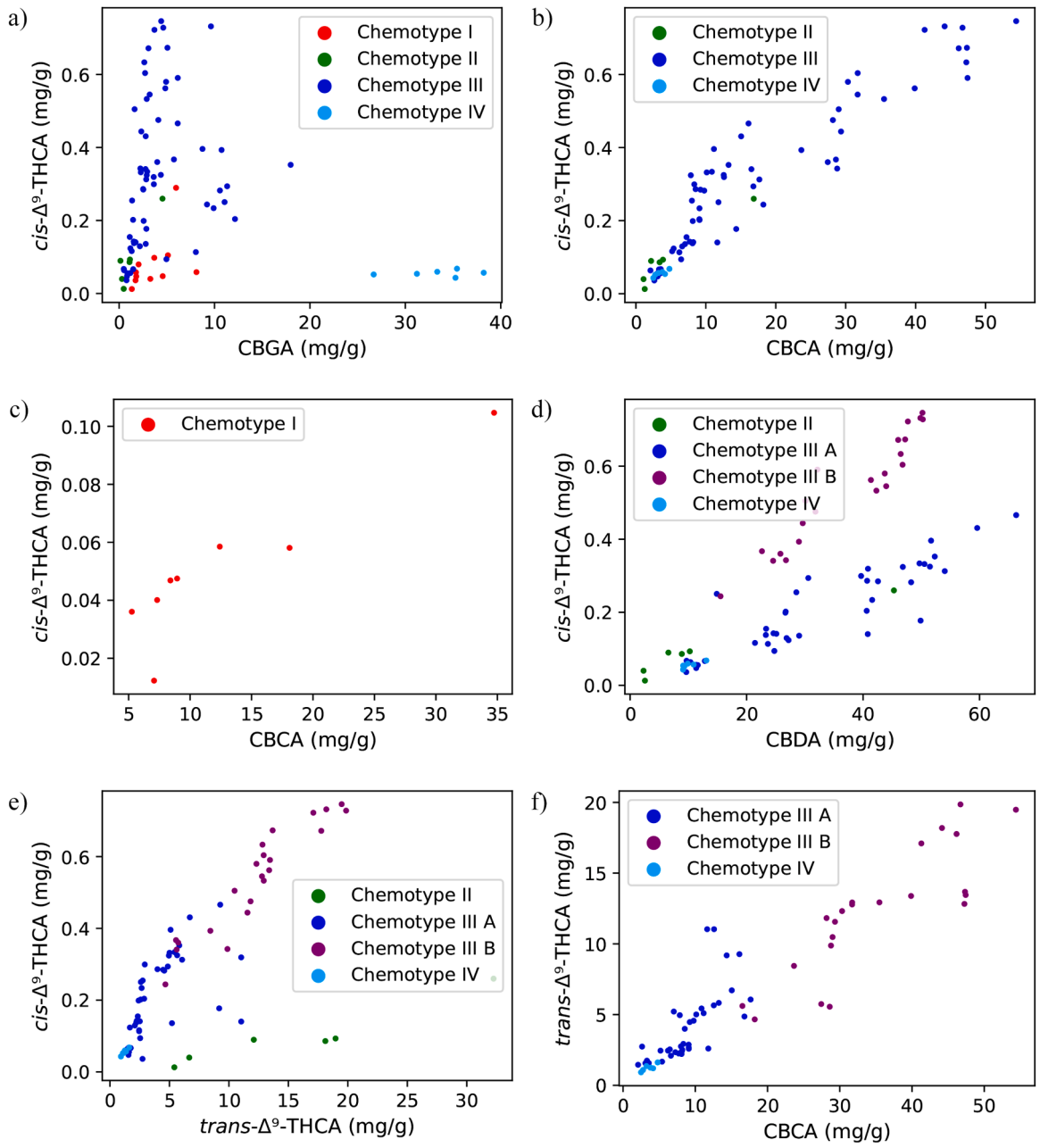

Fig. 5. Phytocannabinoids concentrations relate among themselves with defined trends. 2D Plot of the main phytocannabinoids produced by synthases in cannabis plant compared to *cis*-Δ^9-THCA, in the following order: *cis*-Δ^9-THCA vs CBGA, *cis*-Δ^9-THCA vs *trans*-Δ^9-THCA, *cis*-Δ^9-THCA vs CBCA (for chemotype I samples), *cis*-Δ^9-THCA vs CBDA, *trans*-Δ^9-THCA vs CBCA and *cis*-Δ^9-THCA vs CBCA (for chemotypes II and III samples).

For each phytocannabinoid, relative concentrations were calculated as the ratio between its concentration at a given stage and its maximum concentration in early developmental stages. As expected, CBCA accumulated earliest, peaking at BBCH 11 in chemotype II and at BBCH 12 in chemotypes I and III (Fig. 7). In chemotypes I and III (Fig. 7a, c), *cis*-Δ⁹-THCA and CBCA showed parallel increases, with CBCA consistently accumulating earlier. The peak of *cis*-Δ⁹-THCA was observed slightly later, between BBCH 12 and 13.

In all three chemotypes, *trans*-Δ⁹-THCA and CBDA reached their maximum concentrations at BBCH 13, displaying nearly identical behaviour across stages. Their coincident accumulation patterns reinforce the possibility that these cannabinoids may share enzymatic or regulatory features within the biosynthetic network. The temporal proximity between CBCA and *cis*-Δ⁹-THCA accumulation, together with their strong correlation across samples, is consistent with the hypothesis that *cis*-Δ⁹-THCA may be linked to CBCA biosynthesis.

However, this interpretation remains indirect and does not demonstrate enzymatic causality. Alternative explanations, including shared regulation, parallel biosynthetic pathways, or broader metabolic coupling, cannot be excluded. Among the possible scenarios, the involvement of CBCA synthase (CBCAS) represents a plausible working hypothesis, as *CBCAS* genes are expressed across chemotypes and have been reported to generate secondary or "waste" cannabinoids under certain conditions [27,32–34]. In this context, *cis*-Δ⁹-THCA could potentially arise as a minor side product of CBCAS activity.

It cannot be excluded that *cis*-Δ⁹-THCA is among the so-called "waste cannabinoids". Based on the results of this study, a plausible working hypothesis is that *cis*-Δ⁹-THCA may be produced as a minor side product of CBCA synthase (CBCAS) activity. The genes *CBCAS*, initially defined as *THCAS-like* genes [35], are present in more copies in fiber-type and

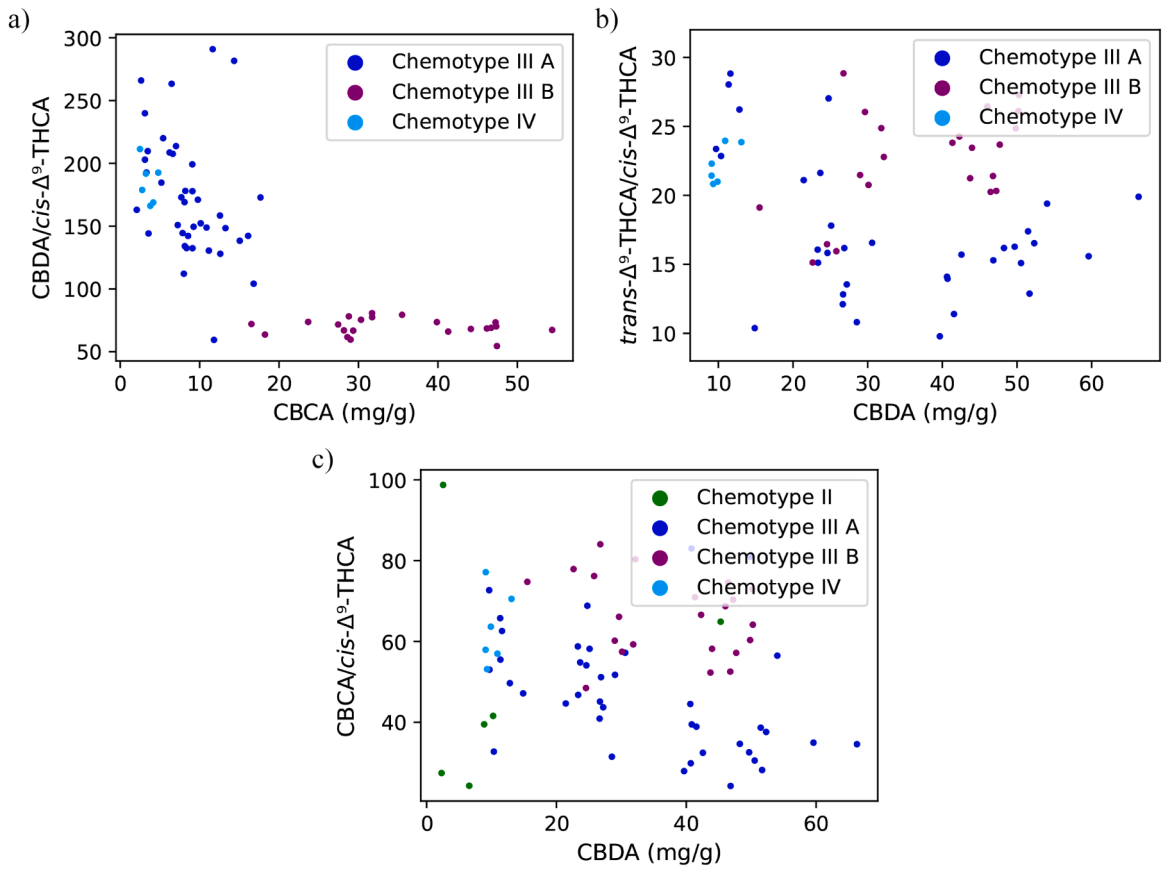

Fig. 6. *cis*-Δ^9-THCA ratio with other phytocannabinoids is independent of CBDA variation. 2D Plot of CBDA and CBCA produced compared to distribution of the ratios among different samples, in the following order: CBDA/*cis*-Δ^9-THCA vs CBCA, *trans*-Δ^9-THCA/*cis*-Δ^9-THCA vs CBDA, CBCA/*cis*-Δ^9-THCA vs CBDA.

drug-type varieties and are also expressed in the inflorescences of all chemotypes [27]. This suggests that CBCAS may not be fully specific, potentially allowing the formation of structurally related minor cannabinoids such as *cis*-Δ⁹-THCA.

The behaviour of *cis*-Δ⁹-THCA across early developmental stages further supports this hypothesis. In our dataset, the accumulation of *cis*-Δ⁹-THCA followed a trend similar to that of CBCA, although with a slight delay, and occurred prior to the maximum accumulation of CBDA and *trans*-Δ⁹-THCA. Considering that CBCAS is strongly expressed during early plant development [29] and has been reported to generate undefined secondary products under certain conditions, these observations are consistent with the possibility that *cis*-Δ⁹-THCA may arise as a minor side product of CBCAS activity. However, this interpretation remains indirect and requires further experimental validation.

In this context, the behaviour of *trans*-Δ⁹-THCA in early-stage chemotype III samples, where THCAS is absent, provides additional support for the hypothesis that *trans*-Δ⁹-THCA may arise as a side product of CBDAS activity in planta. This interpretation is consistent with previous studies reporting the formation of *trans*-Δ⁹-THCA as a secondary product of CBDAS, both *in vitro* [32,33] and in heterologous systems such as *Komagataella phaffii* [34].

The observed developmental trends are also consistent with previous hypotheses suggesting alternative cyclization mechanisms associated with CBCA formation [20], which may extend to carboxylated precursors. Nevertheless, further studies, such as enzymatic assays or heterologous expression systems, will be required to elucidate the precise biochemical mechanism responsible for *cis*-Δ⁹-THCA formation.

Taken together, this study demonstrates that *cis*-Δ⁹-THCA is not an artefactual by-product or a chemical rearrangement derivative but is more likely an intrinsic component of the *C. sativa* metabolome with a specific biosynthetic origin. However, the current evidence is still insufficient to identify the exact biochemical mechanism responsible for its formation.

4. Conclusions

The recently identified phytocannabinoid *cis*-Δ⁹-THCA was shown to share measurable relationships with the three major phytocannabinoids derived from CBGA (CBCA, CBDA, and *trans*-Δ⁹-THCA) although each relationship exhibited chemotype-specific features. These findings are consistent with the possibility that *cis*-Δ⁹-THCA may be formed through an enzymatic process, with a potential involvement of CBCA synthase suggested by the observed correlations in most chemotypes. Notably, THCAS-expressing varieties (chemotypes I and II) showed distinct behaviours in the relationship between Δ^9-THCA isomers, with chemotype II retaining a recognizable correlation and chemotype I showing no measurable trend.

Although the present dataset enabled the formulation of hypotheses regarding the biosynthetic origin of *cis*-Δ⁹-THCA, it does not yet allow definitive conclusions. Additional studies ideally involving controlled enzymatic systems, heterologous expression assays, or compartmentalized models mimicking the trichome environment will be required to elucidate the precise mechanism of formation.

The identification of the acidic precursor *cis*-Δ⁹-THCA provides new insight into previously proposed hypotheses regarding the origin of *cis*-Δ⁹-THC. Earlier studies focused solely on the neutral form and therefore overlooked the native phytocannabinoid composition of the plant. The present results support, but do not demonstrate, the hypothesis of an enzymatic rather than purely chemical origin for *cis*-Δ⁹-THCA. This interpretation is based on (i) the interrelationships observed among phytocannabinoids across a diverse range of chemotypes, and (ii) the comparative analysis of cannabinoid accumulation during early

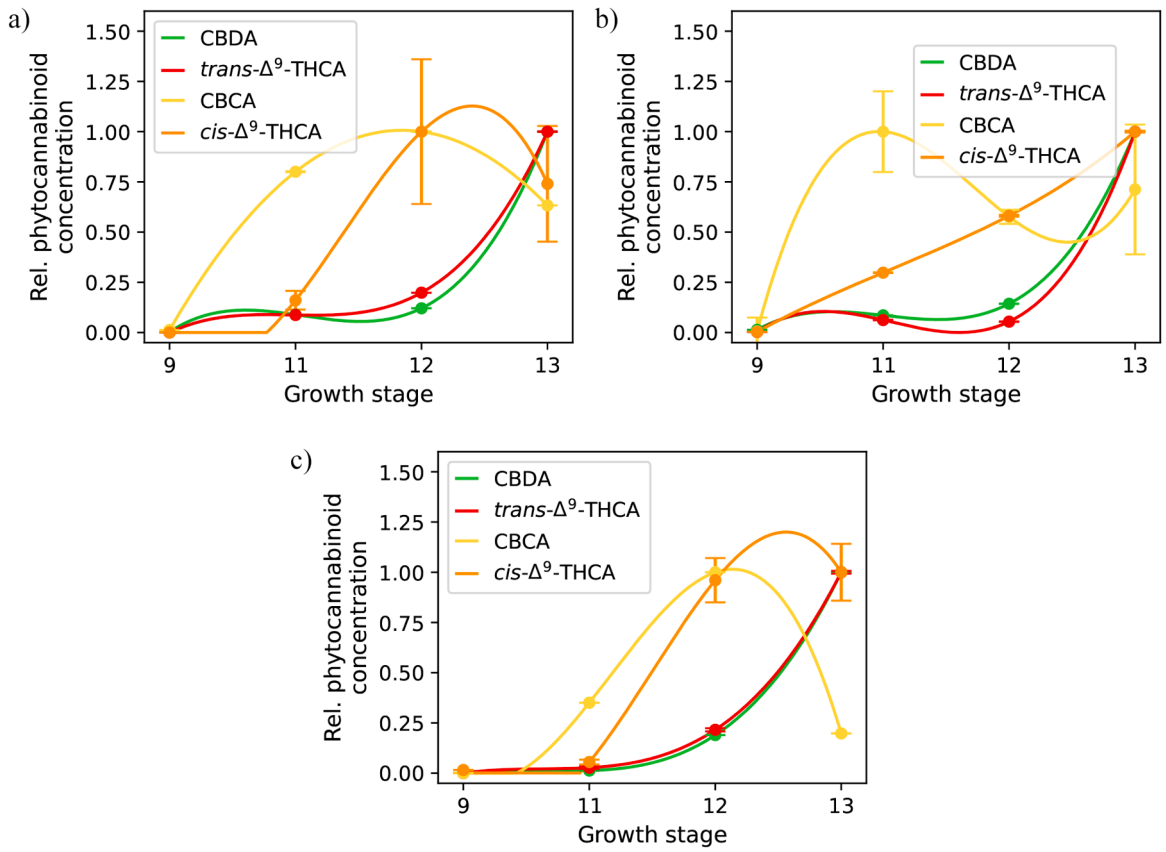

Fig. 7. *cis*-Δ^9-THCA accumulates with a delay after CBCA but before CBDA. Main phytocannabinoids relative concentration across early developmental stages for chemotype I, II and III samples. The values represented are the mean value of each phytocannabinoid for each early-stage sample normalized by the maximum concentration in the early stages and the errors bars are the standard deviation of each concentration normalized by the maximum concentration of each phytocannabinoid in the early stages. The spline is corrected when values are below 0 by assigning them the null value and is only meant for representation purposes.

developmental stages, which offers a temporal perspective on biosynthetic events.

Future investigations integrating chemical, genetic, and biochemical approaches will be essential to define the biosynthetic route responsible for *cis*-Δ^9-THCA formation. Such studies may contribute not only to a deeper understanding of cannabinoid diversity and plant metabolic regulation, but also to potential applications in breeding, biotechnology, and phytocannabinoid production.

Authors' contributions

C.C., G.C. and R.P. contributed to the conception and the design of the research work. L.B. contributed to the acquisition and analysis of the data, together with the scripts for the visualization of the data. L.B., C.C., G.C., R.P., and F.F. contributed to the interpretation of the data and the draft of the work. All authors have contributed to the final revision of the manuscript.

CRediT authorship contribution statement

Giuseppe Cannazza: Writing – review & editing, Writing – original draft, Validation, Supervision, Resources, Project administration, Methodology, Investigation, Funding acquisition, Data curation, Conceptualization. **Cinzia Citti:** Writing – original draft, Validation, Supervision, Methodology, Investigation, Formal analysis, Data curation, Conceptualization. **Ilaria Alberti:** Writing – review & editing, Resources, Data curation. **Flavia Fulvio:** Writing – review & editing, Validation, Investigation. **Roberta Paris:** Writing – review & editing, Resources, Investigation, Data curation, Conceptualization. **Luca Buccolieri:** Writing – review & editing, Writing – original draft, Visualization, Validation, Investigation, Formal analysis.

Funding

This work was funded by UNIHEMP research project "Use of iNdustrIal Hemp biomass for Energy and new biocheMicals Production" (ARS01_00668) funded by Fondo Europeo di Sviluppo Regionale (FESR) (within the PON R&I 2017–2020 – Axis 2 – Action II – OS 1.b). Grant decree UNIHEMP prot. n. 2016 of July 27, 2018; CUP B76C18000520005.

Declaration of Generative AI and AI-assisted technologies in the writing process

During the preparation of this work the authors used Claude from Anthropic (San Francisco, CA, USA) in order to revise the analysis codes. After using this tool/service, the authors reviewed and edited the content as needed and take full responsibility for the content of the article.

Permission for plant material collection

Lines and accessions with a chemotype I and II were cultivated in indoor facilities located in CREA-Research Centre for Cereal and Industrial Crops located in Rovigo (Italy) authorized with decree n. SP/023 on 13th March 2020 according to art. 26 of the D.P.R. 309/90.

Declaration of Competing Interest

The authors declare that they have no known competing financial interests or personal relationships that could have appeared to influence

the work reported in this paper.

Acknowledgements

The authors would like to thank Francesco Tolomeo, former research fellow and now Service Engineer at Thermo Fisher Scientific, for the support in the analysis of the plant samples.

Appendix A. Supporting information

Supplementary data associated with this article can be found in the online version at doi:10.1016/j.jpba.2026.117510.

References

[1] P. Good, A. Haywood, G. Gogna, J. Martin, P. Yates, R. Greer, J. Hardy, Oral medicinal cannabinoids to relieve symptom burden in the palliative care of patients with advanced cancer: a double-blind, placebo controlled, randomised clinical trial of efficacy and safety of cannabidiol (CBD), BMC Palliat. Care 18 (2019) 110, https://doi.org/10.1186/s12904-019-0494-6.

[2] A. Mitelpunkt, U. Kramer, M. Hausman Kedem, E. Zilbershot Fink, R. Orbach, V. Chernuha, A. Fattal-Valevski, L. Deutsch, D. Heffetz, H. Sacks, The safety, tolerability, and effectiveness of PTL-101, an oral cannabidiol formulation, in pediatric intractable epilepsy: A phase II, open-label, single-center study, Epilepsy Behav. 98 (2019) 233–237, https://doi.org/10.1016/j.yebeh.2019.07.007.

[3] M.J. Brodie, P. Czapinski, L. Pazdera, J.W. Sander, M. Toledo, M. Napoles, F. Sahebkar, A. Schreiber, on Behalf of the GWEP1330 Study Group, T. Nezadal, J. Slonkova, A. Altman, K. Füle, Á. Horváth, A. Kelemen, S. Komoly, M. Banach, I. Kurkowska-Jastrzebska, P. Lisewski, M. Falip, R. Rocamora, M. Bagary, A phase 2 randomized controlled trial of the efficacy and safety of cannabidivarin as add-on therapy in participants with inadequately controlled focal seizures, Cannabis Cannabinoid Res 6 (2021) 528–536, https://doi.org/10.1089/can.2020.0075.

[4] D.M. Zylla, J. Eklund, G. Gilmore, A. Gavenda, J. Guggisberg, G. VazquezBenitez, P.A. Pawloski, T. Arneson, S. Richter, A.K. Birnbaum, S. Dahmer, M. Tracy, A. Dudek, A randomized trial of medical cannabis in patients with stage IV cancers to assess feasibility, dose requirements, impact on pain and opioid use, safety, and overall patient satisfaction, Support. Care Cancer 29 (2021) 7471–7478, https://doi.org/10.1007/s00520-021-06301-x.

[5] T. Tajik, K. Baghaei, V.E. Moghadam, N. Farrokhi, S.A. Salami, Extracellular vesicles of cannabis with high CBD content induce anticancer signaling in human hepatocellular carcinoma, Biomed. Pharm. 152 (2022) 113209, https://doi.org/10.1016/j.biopha.2022.113209.

[6] G. Sorrentino, Introduction to emerging industrial applications of cannabis (Cannabis sativa L.), Rend. Lince-.-. Sci. Fis. E Nat. 32 (2021) 233–243, https://doi.org/10.1007/s12210-021-00979-1.

[7] M. Hesami, M. Pepe, A. Baiton, S.A. Salami, A.M.P. Jones, New Insight into Ornamental Applications of Cannabis: Perspectives and Challenges, Plants 11 (2022) 2383, https://doi.org/10.3390/plants11182383.

[8] L.O. Hanuš, S.M. Meyer, E. Muñoz, O. Taglialatela-Scafati, G. Appendino, Phytocannabinoids: a unified critical inventory, Nat. Prod. Rep. 33 (2016) 1357–1392, https://doi.org/10.1039/C6NP00074F.

[9] C. Citti, P. Linciano, S. Panseri, F. Vezzalini, F. Forni, M.A. Vandelli, G. Cannazza, Cannabinoid profiling of hemp seed oil by liquid chromatography coupled to high-resolution mass spectrometry, Front. Plant Sci. 10 (2019) 120, https://doi.org/10.3389/fpls.2019.00120.

[10] C. Citti, P. Linciano, F. Forni, M.A. Vandelli, G. Gigli, A. Laganà, G. Cannazza, Analysis of impurities of cannabidiol from hemp. Isolation, characterization and synthesis of cannabidibutol, the novel cannabidiol butyl analog, J. Pharm. Biomed. Anal. 175 (2019) 112752, https://doi.org/10.1016/j.jpba.2019.06.049.

[11] P. Linciano, C. Citti, F. Russo, F. Tolomeo, A. Laganà, A.L. Capriotti, L. Luongo, M. Iannotta, C. Belardo, S. Maione, F. Forni, M.A. Vandelli, G. Gigli, G. Cannazza, Identification of a new cannabidiol n-hexyl homolog in a medicinal cannabis variety with an antinociceptive activity in mice: cannabidihexol, Sci. Rep. 10 (2020) 22019, https://doi.org/10.1038/s41598-020-79042-2.

[12] P. Linciano, C. Citti, L. Luongo, C. Belardo, S. Maione, M.A. Vandelli, F. Forni, G. Gigli, A. Laganà, C.M. Montone, G. Cannazza, Isolation of a high-affinity cannabinoid for the human CB1 receptor from a medicinal *Cannabis sativa* Variety: Δ^{9} -tetrahydrocannabutol, the butyl homologue of Δ^{9} -tetrahydrocannabinol, J. Nat. Prod. 83 (2020) 88–98, https://doi.org/10.1021/acs.jnatprod.9b00876.

[13] E.B. Russo, H.-E. Jiang, X. Li, A. Sutton, A. Carboni, F. del Bianco, G. Mandolino, D. J. Potter, Y.-X. Zhao, S. Bera, Y.-B. Zhang, E.-G. Lü, D.K. Ferguson, F. Hueber, L.-C. Zhao, C.-J. Liu, Y.-F. Wang, C.-S. Li, Phytochemical and genetic analyses of ancient cannabis from Central Asia, J. Exp. Bot. 59 (2008) 4171–4182, https://doi.org/10.1093/jxb/ern260.

[14] M. Mostafaei Dehnavi, A. Ebadi, A. Peirovi, G. Taylor, S.A. Salami, THC and CBD fingerprinting of an elite cannabis collection from iran: quantifying diversity to underpin future cannabis breeding, Plants 11 (2022) 129, https://doi.org/10.3390/plants11010129.

[15] G. Mazzoccanti, O.H. Ismail, I. D'Acquarica, C. Villani, C. Manzo, M. Wilcox, A. Cavazzini, F. Gasparrini, *Cannabis* through the looking glass: chemo- and enantio-selective separation of phytocannabinoids by enantioselective ultra high performance supercritical fluid chromatography, Chem. Commun. 53 (2017) 12262–12265, https://doi.org/10.1039/C7CC06999E.

[16] F. Russo, F. Tolomeo, M. Angela Vandelli, G. Biagini, A. Laganà, A. Laura Capriotti, A. Cerrato, L. Carbone, E. Perrone, A. Cavazzini, V. Maiorano, G. Gigli, G. Cannazza, C. Citti, Enantioseparation of chiral phytocannabinoids in medicinal cannabis, J. Chromatogr. B 1221 (2023) 123682, https://doi.org/10.1016/j.jchromb.2023.123682.

[17] F. Russo, E. Ferri, D. Pinetti, M.A. Vandelli, A. Laganà, A.L. Capriotti, A. Cavazzini, G. Gigli, C. Citti, G. Cannazza, Bidimensional heart-cut achiral-chiral liquid chromatography coupled to high-resolution mass spectrometry for the separation of the main chiral phytocannabinoids and enantiomerization studies of cannabichromene and cannabichromenic acid, Talanta 267 (2024) 125161, https://doi.org/10.1016/j.talanta.2023.125161.

[18] R.M. Smith, K.D. Kempfert, Δ1-3,4-cis-tetrahydrocannabinol in Cannabis sativa, Phytochemistry 16 (1977) 1088–1089, https://doi.org/10.1016/S0031-9422(00)86745-X.

[19] F. Tolomeo, F. Russo, D. Kaczorova, M.A. Vandelli, G. Biagini, A. Laganà, A. L. Capriotti, R. Paris, F. Fulvio, L. Carbone, E. Perrone, G. Gigli, G. Cannazza, C. Citti, Cis-Δ9-tetrahydrocannabinolic acid occurrence in Cannabis sativa L, J. Pharm. Biomed. Anal. 219 (2022) 114958, https://doi.org/10.1016/j.jpba.2022.114958.

[20] M.A. Schafroth, G. Mazzoccanti, I. Reynoso-Moreno, R. Erni, F. Pollastro, D. Caprioglio, B. Botta, G. Allegrone, G. Grassi, A. Chicca, F. Gasparrini, J. Gertsch, E.M. Carreira, G. Appendino, Δ^{9} - *cis* -Tetrahydrocannabinol: Natural Occurrence, Chirality, and Pharmacology, J. Nat. Prod. 84 (2021) 2502–2510, https://doi.org/10.1021/acs.jnatprod.1c00513.

[21] D.B. Uliss, R.K. Razdan, H.C. Dalzell, G.R. Handrick, Hashish: Synthesis of d1-δ1,6–tetrahydrocannabinol (THC), Tetrahedron Lett. 16 (1975) 4369–4372, https://doi.org/10.1016/S0040-4039(00)91126-2.

[22] R.K. Razdan, B.A. Zitko, Hashish IV: Some acid catalyzed transformations in cannabinoids, Tetrahedron Lett. 10 (1969) 4947–4950, https://doi.org/10.1016/S0040-4039(01)88854-7.

[23] F. Fulvio, L. Righetti, M. Minervini, A. Moschella, R. Paris, The B1080/B1192 molecular marker identifies hemp plants with functional THCA synthase and total THC content above legal limit, Gene 858 (2023) 147198, https://doi.org/10.1016/j.gene.2023.147198.

[24] S. Mishchenko, J. Mokher, I. Laiko, N. Burbulis, H. Kyrychenko, S. Dudukova, Phenological growth stages of hemp (Cannabis sativa L.): codification and description according to the BBCH scale, ŽemėS. Ūkio Moksl 24 (2017), https://doi.org/10.6001/zemesukiomokslai.v24i2.3496.

[25] D. Manns, J. Norwig, K. Reh, Cannabis für medizinische Zwecke: Entwicklung von Arzneibuchmonographien als Qualitätsstandard, Bundesgesundheitsblatt - Gesundh. - Gesundh. 62 (2019) 806–810, https://doi.org/10.1007/s00103-019-02963-5.

[26] P. Linciano, F. Russo, C. Citti, F. Tolomeo, R. Paris, F. Fulvio, N. Pecchioni, M. A. Vandelli, A. Laganà, A.L. Capriotti, G. Biagini, L. Carbone, G. Gigli, G. Cannazza, The novel heptyl phorolic acid cannabinoids content in different Cannabis sativa L. accessions, Talanta 235 (2021) 122704, https://doi.org/10.1016/j.talanta.2021.122704.

[27] F. Fulvio, R. Paris, M. Montanari, C. Citti, V. Cilento, L. Bassolino, A. Moschella, I. Alberti, N. Pecchioni, G. Cannazza, G. Mandolino, Analysis of Sequence Variability and Transcriptional Profile of Cannabinoid synthase Genes in Cannabis sativa L. Chemotypes with a Focus on Cannabichromenic acid synthase, Plants 10 (2021) 1857, https://doi.org/10.3390/plants10091857.

[28] F. Tolomeo, F. Russo, M.A. Vandelli, G. Biagini, A.L. Capriotti, A. Laganà, L. Carbone, G. Gigli, G. Cannazza, C. Citti, HPLC-UV-HRMS analysis of cannabigerovarin and cannabigerobutol, the two impurities of cannabigerol extracted from hemp, J. Pharm. Biomed. Anal. 203 (2021) 114215, https://doi.org/10.1016/j.jpba.2021.114215.

[29] E.P.M. De Meijer, K.M. Hammond, M. Micheler, The inheritance of chemical phenotype in Cannabis sativa L. (III): variation in cannabichromene proportion, Euphytica 165 (2009) 293–311, https://doi.org/10.1007/s10681-008-9787-1.

[30] F. Fulvio, G. Mandolino, C. Citti, N. Pecchioni, G. Cannazza, R. Paris, Phytocannabinoids biosynthesis during early stages of development of young Cannabis sativa L. seedlings: Integrating biochemical and transcription data, Phytochemistry 214 (2023) 113793, https://doi.org/10.1016/j.phytochem.2023.113793.

[31] E. Ferri, F. Russo, M.A. Vandelli, R. Paris, A. Laganà, A.L. Capriotti, A. Gallo, A. Siciliano, L. Carbone, G. Gigli, C. Citti, G. Cannazza, Analysis of phytocannabinoids in hemp seeds, sprouts and microgreens, J. Pharm. Biomed. Anal. 245 (2024) 116181, https://doi.org/10.1016/j.jpba.2024.116181.

[32] K.D. Allen, A. Torres, K. De Cesare, R. Gaudino, Evolution, Expansion and Characterization of Cannabinoid Synthase Gene Family in *Cannabis sativa*, Genomics (2022), https://doi.org/10.1101/2022.11.18.517131.

[33] F. Thomas, O. Kayser, Natural deep eutectic solvents enhance cannabinoid biotransformation, Biochem. Eng. J. 180 (2022) 108380, https://doi.org/10.1016/j.bej.2022.108380.

[34] B. Zirpel, O. Kayser, F. Stehle, Elucidation of structure-function relationship of THCA and CBDA synthase from Cannabis sativa L, J. Biotechnol. 284 (2018) 17–26, https://doi.org/10.1016/j.jbiotec.2018.07.031.

[35] M. Kojoma, H. Seki, S. Yoshida, T. Muranaka, DNA polymorphisms in the tetrahydrocannabinolic acid (THCA) synthase gene in "drug-type" and "fiber-type" Cannabis sativa L, Forensic Sci. Int. 159 (2006) 132–140, https://doi.org/10.1016/j.forsciint.2005.07.005.